

# Disk Substructures at High Angular Resolution Project (DSHARP): X. Gaps and Rings with Planet Scenario

S. ZHANG, Z. ZHU, ...<sup>1</sup>

<sup>1</sup>Department of Physics and Astronomy, University of Nevada, Las Vegas, 4505 S. Maryland Pkwy, Las Vegas, NV, 89154, USA

## ABSTRACT

TBD

**Keywords:** circumstellar matter — planetary systems: formation, protoplanetary disks — dust

## 1. INTRODUCTION

generic background: to understand planet formation, we need to find young forming planets in protoplanetary disks. However, direct detection is difficult and we only have 6 candidates so far. Indirect methods which use disk features induced by planet-disk interaction can be efficient at probing young planets.

Planet-disk interaction has been studied thoroughly over the past three decades. Analytical models, 2 dimensional, 3 dimensional models have all been developed. However, earlier works focus on planet migration and gap opening. Only very recently, with the striking ALMA images, people have started to focus on studying the detectability of disk features due to planet-disk interaction. Most efforts have been studying features from dust scattering (near-IR scattered light images, submm polarization) or dust thermal emission (submm emission). Recently, people start to use gas kinematics to probe planets (sub/super Keplerian motion and velocity kinks ).

Among all these methods, probing dust submm emission is still the most sensitive method to low mass planets since change in little gas surface density can cause dramatic dust surface density change. However, there is huge degeneracy and a lot of mechanisms can cause dust rings/gaps, such as ice lines, dead zone transition, MHD zonal flows, dust gravitational instability, resonances with planets, etc.

However, there is no systematic study on thermal emission features due to planet-disk interaction among different disk properties and planet properties. In this work, we did such parameter study. Our work differs from previous work in several aspects.

We include the dust drift. We consider opacity at 1.3 mm, the same as ALMA runs in this large program.

## 2. METHOD

We carried out 2-D hydrodynamical simulations using the modified version of the grid-based code FARGO, called FARGO-particle. It simulates gas hydrodynamics using finite difference method, while simulate the dust dynamics using Lagrangian particle method.

### 2.1. Setup: Gas and Dust

To represent the surface density of a realistic disk, we initialize the gas surface density as

$$\Sigma(r) = \Sigma_0(R/R_0)^{-1}, \quad (1)$$

where  $R_0 = 1$ , is the position of the planet. We assume Isothermal EOS, the gas grid is under polar coordinate  $(R, \theta)$  ranging from 0.1 to  $10 R_0$  in radial direction and 0 to  $2\pi$  in  $\theta$  direction. For the viscosity  $\alpha = 10^{-4}$  and  $10^{-3}$  runs, the grids are  $750 \times 1024$  in  $(R, \theta)$  directions, and  $375 \times 512$  for  $\alpha = 10^{-2}$  runs. resolution, boundary condition, indirect force, smoothing length, (basically parameters in the input file.)...

The dust's total surface density is 1/100 of the gas surface density, initially. But both gas and dust can be accreted out of the boundaries. Thus at the end of the day, the dust-to-gas ratio might not be 1/100.

No disk self-gravity, no gas gravity from gas to dust. no feedback. All these to ensure that we can scale the simulations.

The dust particles are much smaller than the molecular mean-free path in our disk model so that the drag force experienced by the particles is in the Epstein regime. The dimensionless stopping time

$$St = t_s \Omega = \frac{\pi}{2} \frac{s \rho_p}{\Sigma_{gas}} \quad (2)$$

If we use  $\rho_p = 1 g cm^{-3}$ , we have

$$St = \dots \quad (3)$$

We use x0,000 particles. (400, 000 for alpha = 1e-4 and 1e-3, 200, 000 for alpha = 1e-2) Each particle is a super particle. The dust size distribution in the simulation is set to be

$$n(a) = a^{-p} \quad (4)$$

where  $p = 4$ . But the dust size distribution can be scaled to any desired power-law, say,  $p = 3.5$ , as the case in ISM. . particle turbulent diffusion.

## 2.2. Grid of Models

We chose three h/r ( $h/r=0.05, 0.07, 0.1$ ), 5 planet mass ( $3.3 \times 10^{-5}, 10^{-4}, 3.3 \times 10^{-4}, 10^{-3}, 3.3 \times 10^{-3} M_{\odot}$  or roughly  $11 M_{\oplus}, 33 M_{\oplus}, 0.35 M_J, 1 M_J, 3.5 M_J$ ), and 3 disk viscosity  $\alpha$  ( $\alpha = 0.01, 0.001, 0.0001$ ).

The reason to choose these parameters....

Acronym h5am3p1 means  $h/r=0.05, \alpha = 10^{-3}, M_p = 3.3 \times 10^{-5} M_{\odot}$ . (If we assume the central star is one solar mass. Otherwise  $M_p/M_* = 3.3 \times 10^{-5}$ .)

## 2.3. Calculating the Intensity at Submm

How to scale the simulation results to real systems with a given star mass, luminosity, and surface density?

1) calculate the gas temperature using the new fitting formula.

2) use the estimated gas surface density to calculate how the particles size in real systems corresponds to particles in simulations.

3) Using the assumed particle size distribution in real system to calculate the mass weight for each particles in the simulation.

4) Add the opacity for each sized particle to derive the total optical depth.

5) Calculate  $1 - \exp(-\tau)$ , and derive the brightness temperature.

(With the assumption that  $T(r) \propto r^{-0.5}$ )

## 3. SIMULATION RESULTS

### 3.1. Gas

The azimuthally averaged gas surface density at  $t=100 T_0$  for  $h/r=0.05, 0.07$ , and  $0.1$  cases are shown in Figure 1.

1) When the planet mass increases, the gap depth normally increases. However, when the gap is eccentric (e.g. h5am4p5, h5am3p5), the azimuthally averaged gas surface density is actually higher than the case with lower mass planets. This is purely due to the averaging process.

2) With the same planet mass, gaps in  $h/r=0.1$  cases are shallower but wider than the  $h/r=0.05$  cases. This is consistent with previous studies (Kanagawa et al. 2015, 2016).

3) With the same planet mass, the same  $h/r$ , the gaps are shallower with increasing  $\alpha$ .

4) The gap edge becomes smoother with increasing  $\alpha$ . With  $\alpha = 0.01$ , the gap edge is very smooth. With  $\alpha = 10^{-3}$ , the gap edge increases a little bit. With  $\alpha = 10^{-4}$ , clearly we see two spikes at the gap edge.

5) For  $\alpha = 10^{-4}$  cases, we see multiple rings as in recent papers.

The two-dimensional contours in Figure 2 show a lot of details on the azimuthal structure of the disk.

### 3.2. Dust and Thermal Emission

Since dust to gas feedback is assumed to be not important, we can scale our dust distribution to match any

system. To explore how different dust size distribution can affect the final intensity images, we choose two very different dust size distribution to explore the effect. In one case, we assume  $n(s) \propto s^{-3.5}$  with the maximum grain size of 0.55 mm in the initial condition. And in the other case, we assume  $n(s) \propto s^{-2}$  with the maximum grain size of 5.5 mm. The shallower dust size distribution is consistent with SED constraints (D'Alessio et al. 2001). The shallower slope and the bigger particle size explore the scenario that dust has grown in protoplanetary disks already.

The intensity for these two dust size distributions are shown in Figures 3 and 4.

With bigger particles, the gap edge is definitely sharper and forming a narrower ring. The larger the  $\alpha$  is, the rings are wider.

Several non-axisymmetric structures to notice:

1) The gaps in the lower left plots (h5am4p5, h5am3p5) are eccentric. Eccentric gaps only show up with massive planets. So maybe we can use gap eccentricity to constrain the planet mass.

2) For the lowest viscosity case ( $\alpha = 10^{-4}$ ), vortices can appear at the gap edge. Even a  $30 M_{\odot}$  planet can induce the vortex. The vortex sometimes is inside the gap edge. (probably it concentrates smaller particles while bigger particles are trapped outside further away at the gap edge. Needs to be checked)

3) The dust concentration at L4 or L5 or both L4/L5 is seen in some  $\alpha = 10^{-4}$  cases.

Since the same sized particle has different dynamical properties (stokes number) with different disk gas surface density. We have explored three gas surface densities ( $0.1, 1, 10 g/cm^2$ ). (We have  $0.1, 0.3, 1, 3, 10, 30, 100 g/cm^2$ . Three are shown in Fig. 5.)

The profiles of the models in  $smax = 5.5$  mm is more alike  $smax = 0.55$  mm at gas density 10 times smaller. (ex.  $smax=5.5$  mm,  $\Sigma_g = 100 g/cm^2$  is similar to  $smax=0.55$  mm,  $\Sigma_g = 10 g/cm^2$ .)

## 4. FITTING GAPS/RINGS

Dong & Fung (2017) Kanagawa et al. (2016) are not applicable here.

They both consider gas, even dong find a mapping from gas density to intensity. They do not consider dust trapping. The dust trapping would brighten the outer edge and lower the bottom of the gap.

Dong & Fung (2017) deal with

So we use a new definition, which is similar to Kanagawa et al. (2016)

For the gas, we fit the gas density. For the dust, we fit the temperature profile. (More specifically,  $r^{-0.5} (1 - e^{-\tau})$ .)

We first find the outer peak. (This is where dust piles up due to the dust trapping.) and mark this point as  $r_{peak}$ , and we find the bottom of the gap left to /inside of  $r_{peak}$  and mark it as  $r_{gap}$ . If there are horseshoe around  $R=1$ , we will cross through the horseshoe and treat two

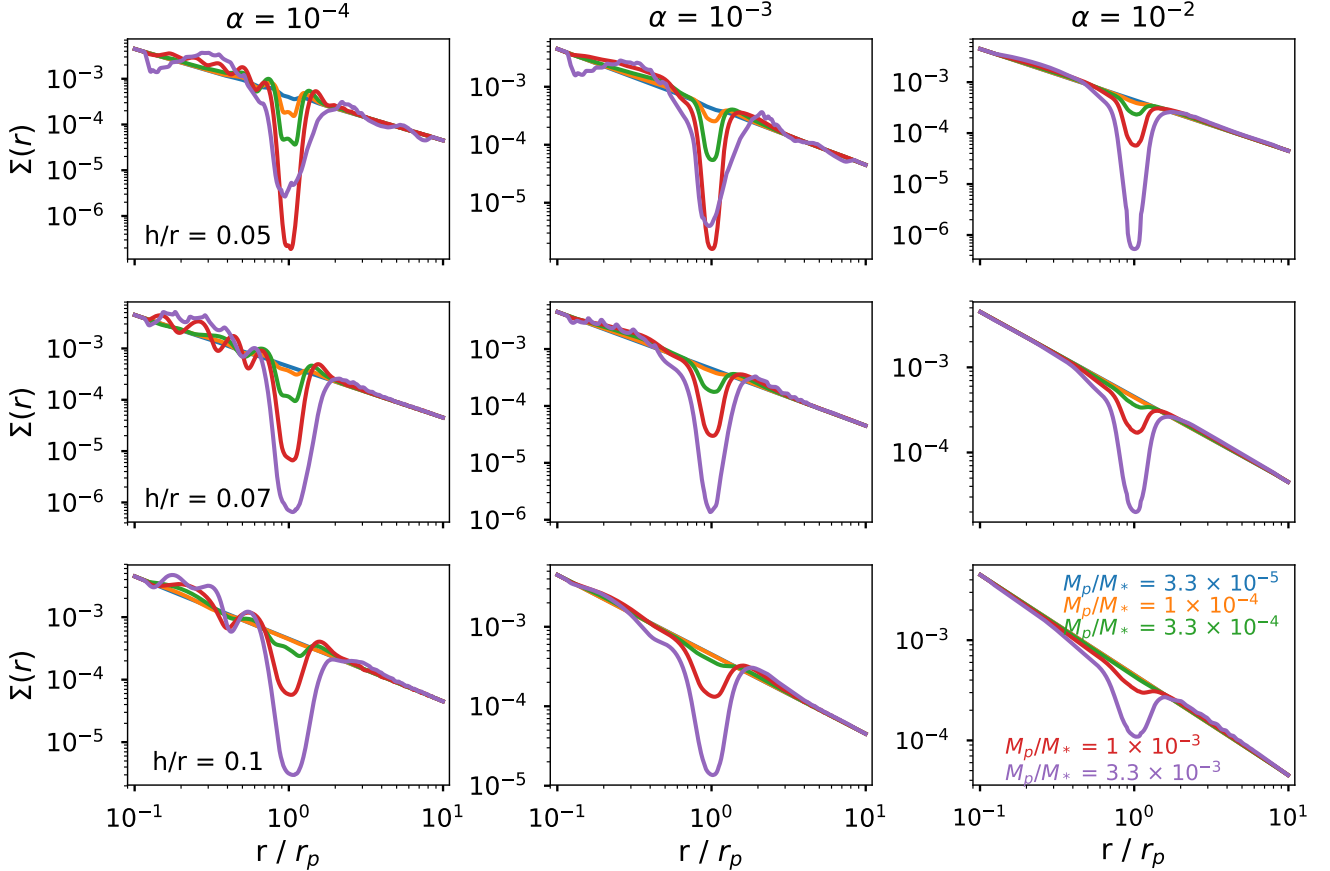


**Figure 1.** The gas surface density for  $h/r=0.05$  cases (upper panels) and  $h/r=0.1$  cases (bottom panels). From left to right,  $\alpha = 10^{-4}, 10^{-3}, 10^{-2}$  in disks. Different colors represent planets having different masses.

individual (We'll later separate these two gaps and mark them individually. Thus will give both the "total gap widths" and the individual gap widths for cases that have horseshoes.)

We define the gap depth  $\delta$  as

$$\delta = I(r_{peak})/I(r_{gap}) \quad (5)$$

where  $I$  defines the intensity profile of the dust or for gas  $\delta = \Sigma(r_{peak}) / \Sigma(r_{gap})$ , where  $\Sigma$  denotes the gas surface density profile.

Then similar to Kanagawa16, we calculate the edge intensity (or edge density for gas.) as

$$I_{edge} = (I(r_{peak}) + I(r_{gap}))/2 \quad (6)$$

We find two edges  $r_{in}$  at the inner disk and  $r_{out}$  at the outer disk, where  $I(r_{in}) = I(r_{out}) = I_{edge}$ .

Then we define the gap widths  $\Delta$  as,

$$\Delta = (r_{out} - r_{in})/r_{out} \quad (7)$$

Kanagawa+16's definition  $\Delta = r_{out} - r_{in}$  is not consistent between their simulation and observation. They

use rout-rin in their simulation, but rout-rin/rmid in examples from observation. Because in observation we don't know where is the planet, so we can't use rout-rin. Our method is consistent. (Even though rout-rin gives us tightest liner relation.) Thus this method is better for deep gap. At least there is a local maxima in the 1d profile.

Say, if there is a shallow gap which can be spotted by eye, but the profile decreases all the way throughout the gap region. just the slope becomes larger at inner gap and becomes smaller at out edge, out prescription cannot find it.

Table. 1 summarizes our fitting results. (Now only contains gas gap widths and dust gap widths for smax=550um and p=-3.5. will update once the opacity is finalized.)

$$\delta = I(r_{gap})/I(r_{peak}) \quad (8)$$

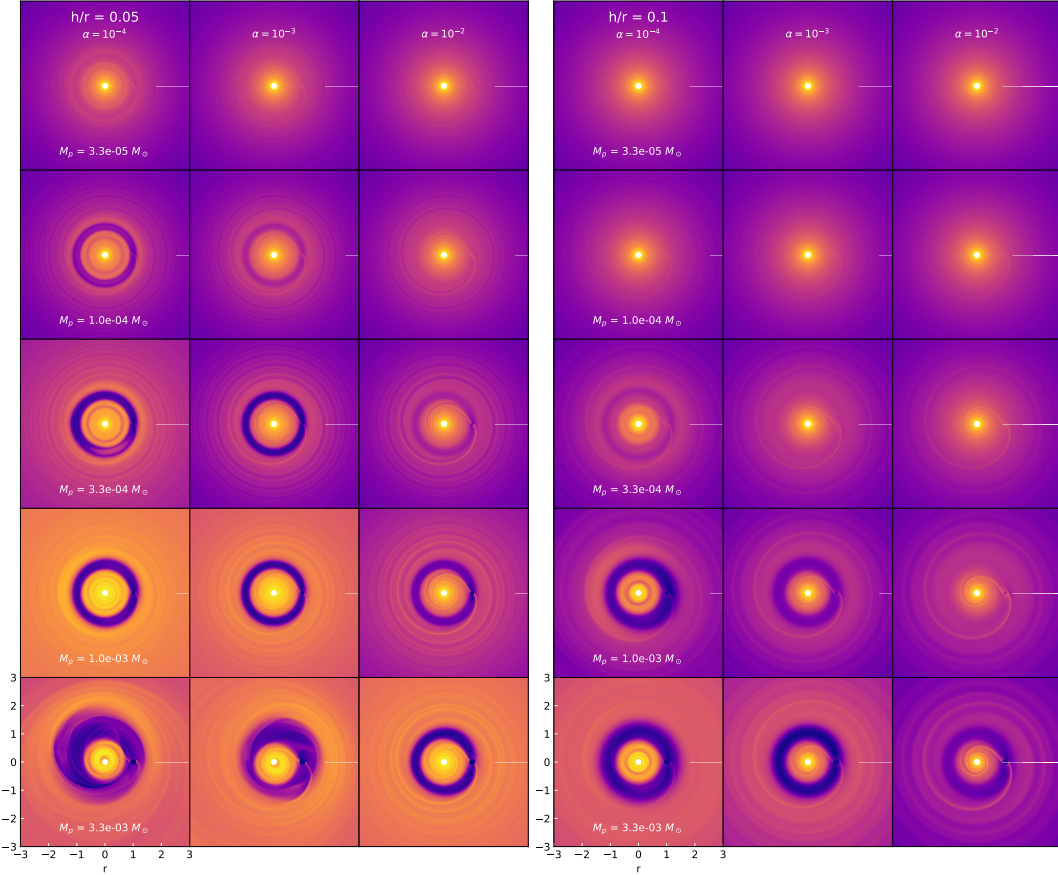


**Figure 2.** The gas surface density in log scale for  $h/r=0.05$  cases (upper panels) and  $h/r=0.1$  cases (bottom panels). From left to right,  $\alpha = 10^{-4}, 10^{-3}, 10^{-2}$  in disks. The planet mass increases from top to bottom

**Table 1.** Gap Width smax=550 um, slope = -3.5

$h/r$ (1)	$\alpha$ (2)	$q$ (3)	$\Delta_g$ (4)	$\Delta_{d,0p1}$ (5)	$\Delta_{d,0p3}$ (6)	$\Delta_{d,1}$ (7)	$\Delta_{d,3}$ (8)	$\Delta_{d,10}$ (9)	$\Delta_{d,30}$ (10)	$\Delta_{d,100}$ (11)
0.05	$10^{-4}$	$3.3 \times 10^{-5}$	0.09	0.90	0.76	0.56	0.28	0.18	0.11	0.00
0.05	$10^{-4}$	$1 \times 10^{-4}$	0.24	1.00	0.96	0.72	0.53	0.24	0.20	0.00
0.05	$10^{-4}$	$3.3 \times 10^{-4}$	0.32	1.00	0.96	0.72	0.38	0.28	0.09	0.05
0.05	$10^{-4}$	$1 \times 10^{-3}$	0.42	1.00	1.00	0.62	0.45	0.39	0.15	0.11
0.05	$10^{-4}$	$3.3 \times 10^{-3}$	0.55	1.00	0.75	0.70	0.57	0.94	0.46	0.37
0.05	$10^{-3}$	$3.3 \times 10^{-5}$	0.00	0.00	0.00	0.15	0.12	0.10	0.00	0.00
0.05	$10^{-3}$	$1 \times 10^{-4}$	0.20	1.00	0.98	0.66	0.38	0.21	0.14	0.00
0.05	$10^{-3}$	$3.3 \times 10^{-4}$	0.27	1.00	0.93	0.66	0.46	0.31	0.20	0.13
0.05	$10^{-3}$	$1 \times 10^{-3}$	0.37	1.00	0.83	0.65	0.52	0.39	0.30	0.21

*Table 1 continued*

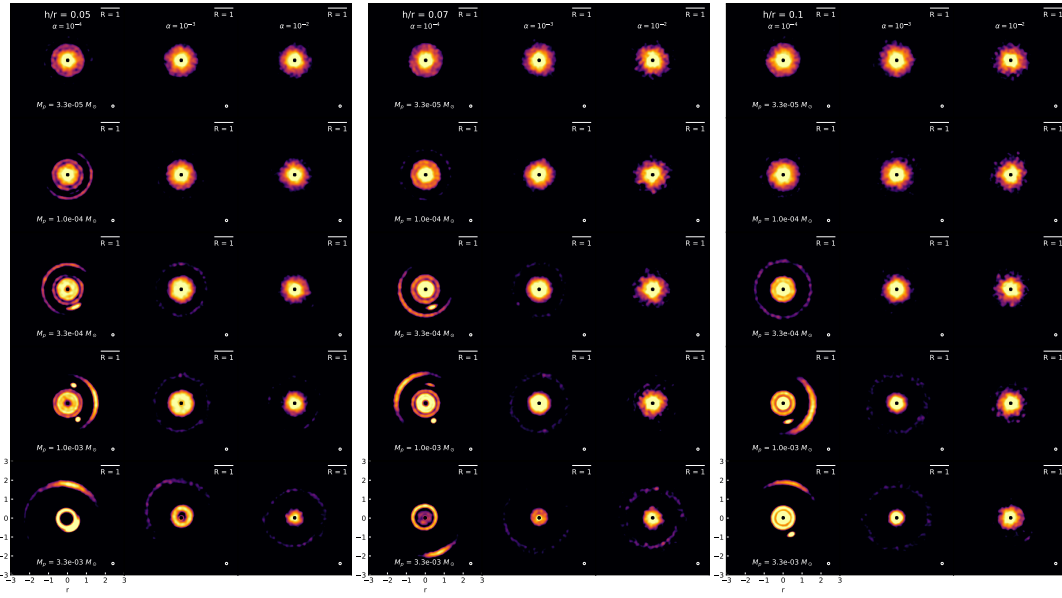


**Figure 3.** The intensity contours for cases with  $h/r=0.05$  (left panels),  $h/r=0.07$  (middle panels) and  $h/r=0.1$  (right panels). The initial gas surface density at the planet position is  $3 \text{ g cm}^{-2}$ . From left to right,  $\alpha = 10^{-4}, 10^{-3}, 10^{-2}$  in disks. From top to bottom, the planet masses increases. The initial dust size distribution follows  $n(s) \propto s^{-3.5}$  with the maximum grain size of  $100 \mu\text{m}$ .

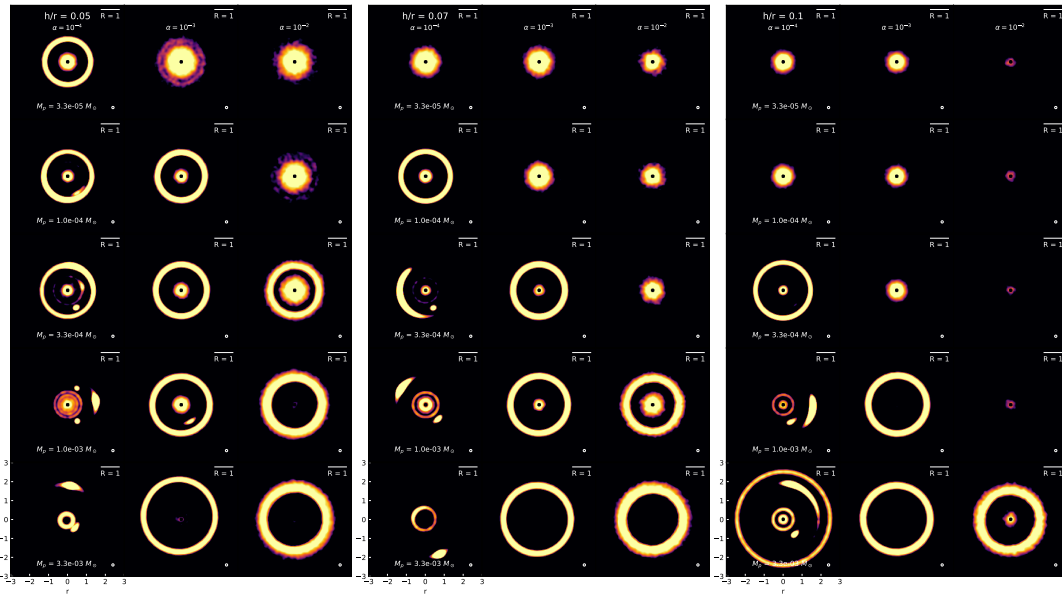


**Figure 4.** Similar to Figure 4, except that the initial dust size distribution is assumed to follow  $n(s) \propto s^{-2.5}$  with the maximum grain size of  $1 \text{ cm}$ .

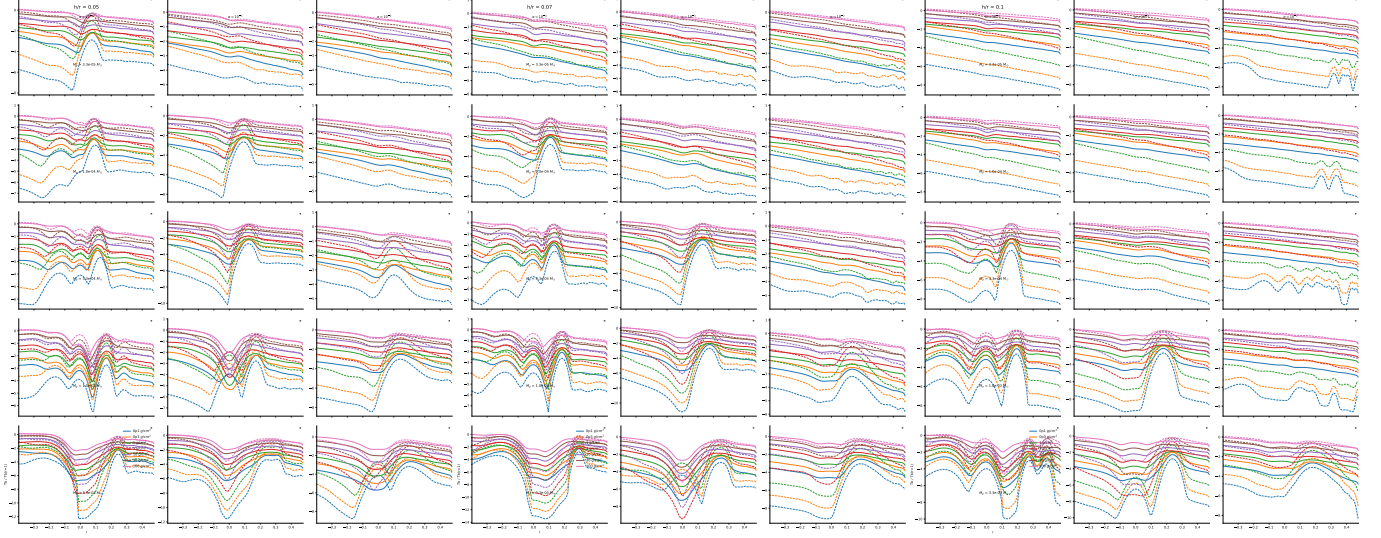


**Figure 5.** The radial intensity for cases with  $h/r=0.05$  (left panels) and  $h/r=0.1$  (right panels). The initial gas surface density at the planet position is  $10 \text{ g cm}^{-2}$ . From left to right,  $\alpha = 10^{-4}, 10^{-3}, 10^{-2}$  in disks. From top to bottom, the planet masses increases. The upper three have the initial dust size distribution of  $n(s) \propto s^{-3.5}$  with the maximum grain size of 0.55 mm. The lower three have the initial dust size distribution of  $n(s) \propto s^{-2}$  with the maximum grain size of 5.5 mm.

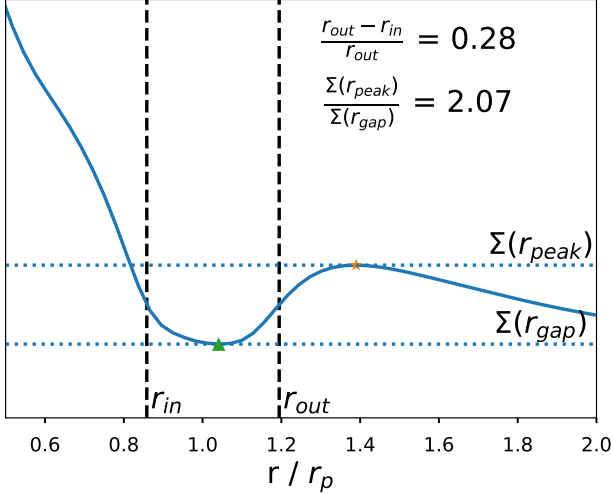


**Figure 6.** An example of the definition of gap depth ( $\delta$ ) and width ( $\Delta$ ).  $r_{peak}$  (marked by a star) and  $r_{gap}$  (marked by a triangle) are first found and are used to calculate  $\Sigma_{edge}$ , which is the average of  $\Sigma(r_{peak})$  and  $\Sigma(r_{gap})$ . (For dust,  $I_{edge} = (I(r_{peak}) + I(r_{gap})) / 2$ .) The gap width  $\Delta$  is the difference between the values of two vertical dashed line divided by position of outer dashed line  $r_{out}$ , namely  $(r_{out}-r_{in})/r_{out}$ . The depth is  $\Sigma(r_{peak})/\Sigma(r_{gap})$ , which is indicated by two horizontal dotted lines. Note that we fit gap widths and depths of gas using gas surface density  $\Sigma_g(r)$  and fit the gap widths and depths of dust using dust intensity profile  $I(r)$ . (This example is taken from gas density profile of the model *outh0p07a1em3p2*.)

**Table 1** (*continued*)

h/r	$\alpha$	q	$\Delta_g$	$\Delta_{d,0p1}$	$\Delta_{d,0p3}$	$\Delta_{d,1}$	$\Delta_{d,3}$	$\Delta_{d,10}$	$\Delta_{d,30}$	$\Delta_{d,100}$
(1)	(2)	(3)	(4)	(5)	(6)	(7)	(8)	(9)	(10)	(11)

**Table 1** (*continued*)

h/r	$\alpha$	q	$\Delta_g$	$\Delta_{d,0p1}$	$\Delta_{d,0p3}$	$\Delta_{d,1}$	$\Delta_{d,3}$	$\Delta_{d,10}$	$\Delta_{d,30}$	$\Delta_{d,100}$
(1)	(2)	(3)	(4)	(5)	(6)	(7)	(8)	(9)	(10)	(11)

**Table 1** (*continued*)

h/r	$\alpha$	q	$\Delta_g$	$\Delta_{d,0p1}$	$\Delta_{d,0p3}$	$\Delta_{d,1}$	$\Delta_{d,3}$	$\Delta_{d,10}$	$\Delta_{d,30}$	$\Delta_{d,100}$
(1)	(2)	(3)	(4)	(5)	(6)	(7)	(8)	(9)	(10)	(11)
0.05	$10^{-3}$	$3.3 \times 10^{-3}$	0.57	1.00	0.92	0.90	0.60	0.50	0.38	0.29
0.05	$10^{-2}$	$3.3 \times 10^{-5}$	0.00	0.00	0.00	0.00	0.00	0.00	0.00	0.00
0.05	$10^{-2}$	$1 \times 10^{-4}$	0.00	0.00	0.00	0.00	0.00	0.00	0.00	0.00
0.05	$10^{-2}$	$3.3 \times 10^{-4}$	0.21	0.62	0.52	0.30	0.23	0.17	0.00	0.00
0.05	$10^{-2}$	$1 \times 10^{-3}$	0.30	1.00	1.00	0.86	0.52	0.32	0.22	0.00
0.05	$10^{-2}$	$3.3 \times 10^{-3}$	0.43	1.00	1.00	0.71	0.56	0.39	0.27	
0.07	$10^{-4}$	$3.3 \times 10^{-5}$	0.00	0.00	0.00	0.00	0.10	0.11	0.07	0.00
0.07	$10^{-4}$	$1 \times 10^{-4}$	0.14	1.00	0.90	0.71	0.43	0.29	0.16	0.00
0.07	$10^{-4}$	$3.3 \times 10^{-4}$	0.33	1.00	1.00	0.80	0.66	0.34	0.11	0.06
0.07	$10^{-4}$	$1 \times 10^{-3}$	0.42	1.00	0.79	0.75	0.61	0.42	0.36	0.11
0.07	$10^{-4}$	$3.3 \times 10^{-3}$	0.56	1.00	1.00	0.66	0.61	0.58	0.52	0.44
0.07	$10^{-3}$	$3.3 \times 10^{-5}$	0.00	0.00	0.00	0.00	0.00	0.00	0.00	0.00
0.07	$10^{-3}$	$1 \times 10^{-4}$	0.00	0.00	0.00	0.00	0.17	0.14	0.00	0.00
0.07	$10^{-3}$	$3.3 \times 10^{-4}$	0.28	1.00	1.00	0.77	0.58	0.32	0.22	0.13
0.07	$10^{-3}$	$1 \times 10^{-3}$	0.36	1.00	1.00	0.77	0.62	0.45	0.32	0.21
0.07	$10^{-3}$	$3.3 \times 10^{-3}$	0.52	1.00	1.00	1.00	0.85	0.63	0.47	0.35
0.07	$10^{-2}$	$3.3 \times 10^{-5}$	0.00	0.00	0.00	0.00	0.00	0.00	0.00	0.00
0.07	$10^{-2}$	$1 \times 10^{-4}$	0.00	0.00	0.00	0.00	0.00	0.00	0.00	0.00
0.07	$10^{-2}$	$3.3 \times 10^{-4}$	0.00	0.00	0.00	0.00	0.00	0.00	0.00	0.00
0.07	$10^{-2}$	$1 \times 10^{-3}$	0.28	0.76	0.72	0.41	0.34	0.11	0.00	0.00
0.07	$10^{-2}$	$3.3 \times 10^{-3}$	0.40	1.00	1.00	1.00	0.82	0.47	0.34	0.00
0.10	$10^{-4}$	$3.3 \times 10^{-5}$	0.00	0.00	0.00	0.00	0.00	0.07	0.00	0.00
0.10	$10^{-4}$	$1 \times 10^{-4}$	0.00	0.00	0.00	0.00	0.00	0.09	0.08	0.00
0.10	$10^{-4}$	$3.3 \times 10^{-4}$	0.21	1.00	1.00	0.82	0.56	0.45	0.23	0.00
0.10	$10^{-4}$	$1 \times 10^{-3}$	0.41	1.00	1.00	0.84	0.76	0.49	0.41	0.31
0.10	$10^{-4}$	$3.3 \times 10^{-3}$	0.53	1.00	0.89	0.86	0.72	0.70	0.68	0.25
0.10	$10^{-3}$	$3.3 \times 10^{-5}$	0.00	0.00	0.00	0.00	0.00	0.00	0.00	0.00
0.10	$10^{-3}$	$1 \times 10^{-4}$	0.00	0.00	0.00	0.00	0.00	0.00	0.00	0.00
0.10	$10^{-3}$	$3.3 \times 10^{-4}$	0.00	0.00	0.00	0.00	0.13	0.16	0.00	0.00
0.10	$10^{-3}$	$1 \times 10^{-3}$	0.38	1.00	1.00	1.00	0.73	0.49	0.36	0.00
0.10	$10^{-3}$	$3.3 \times 10^{-3}$	0.49	1.00	1.00	1.00	0.80	0.64	0.49	0.37
0.10	$10^{-2}$	$3.3 \times 10^{-5}$	0.00	0.00	0.00	0.00	0.00	0.00	0.00	0.00
0.10	$10^{-2}$	$1 \times 10^{-4}$	0.00	0.00	0.00	0.00	0.00	0.00	0.00	0.00
0.10	$10^{-2}$	$3.3 \times 10^{-4}$	0.00	0.00	0.00	0.00	0.00	0.00	0.00	0.00
0.10	$10^{-2}$	$1 \times 10^{-3}$	0.11	0.00	0.00	0.00	0.00	0.00	0.00	0.00
0.10	$10^{-2}$	$3.3 \times 10^{-3}$	0.38	1.00	0.99	0.67	0.43	0.19	0.09	0.00

NOTE—A summary of widths of models. Some of them have multiple gaps. Will also treat them separately later.

After we have fitted all the widths and depths of gaps. We try to find a relation between the gap widths, depths and h/r, alpha, q motivated by Kanagawa+1516 and DongFung.

We first use this method to fit the gas density profile. and find a relationship

$$K' = q(h/r)^{-0.18} \alpha^{-0.31} \quad (9)$$

(In Kanagawa's notation it's  $K' = q^2(h/r)^{-0.36} \alpha^{-0.63}$ ).

Then we find the best linear fit. Eliminating the outliers by criteria as follows. (1) The gap width should be larger than... (2) if it's just open a very narrow gap in the series alpha = 1e-4, 1e-3, 1e-2 or h/r = 0.05, 0.07, 0.1...

$$\Delta = AK'^B \quad (10)$$

Where A and B is a function of gas density at the planet position and dust size distribution.

As for the depth, Kanagawa+15 has an analytical derivation.

$$K = q^2(h/r)^{-5}\alpha^{-1} \quad (11)$$

and

$$\delta - 1 = 0.04K \quad (12)$$

DongFung also uses this. We find  
Our constant is 0.01

Haven't started to do this part.

Note that since depths is more sensitive to the convolution beam, we use widths first and then use depths to help us constrain planet mass.

We derive the gap depth and width in the intensity image for all cases.

We apply those to LP sources to derive the potential planet mass. We will do for all gaps. But we will caution that the deeper and wider gaps have higher chances to be associated with planets.

## 5. DISCUSSION

### 5.1. *The Smallest Planets Probed by ALMA*

We will explore what mass planets can be probed by ALMA. Provide the detection limit using dust continuum.

### 5.2. *Our Solar System and HR 8799 in Taurus*

If we put our solar system and HR 8799 in Taurus, how they look like?

## 6. CONCLUSION

## 7. APPENDIX

The fitting formula for all the gaseous gaps.

## REFERENCES

Dong, R., & Fung, J. 2017, ApJ, 835, 146,  
doi: [10.3847/1538-4357/835/2/146](https://doi.org/10.3847/1538-4357/835/2/146)

Kanagawa, K. D., Muto, T., Tanaka, H., et al. 2016, PASJ, 68, 43, doi: [10.1093/pasj/psw037](https://doi.org/10.1093/pasj/psw037)

**Table 2.** The relation between gap width  $\Delta$  and  $K'$ 

Parameters	$\Delta_g$	$\Delta_{d,0p1}$	$\Delta_{d,0p3}$	$\Delta_{d,1}$	$\Delta_{d,3}$	$\Delta_{d,10}$	$\Delta_{d,30}$	$\Delta_{d,100}$
(1)	(2)	(3)	(4)	(5)	(6)	(7)	(8)	(9)
A	1.05	-	-	1.53	1.60	1.81	1.29	1.08
B	0.26	-	-	0.18	0.27	0.36	0.34	0.39

NOTE— $\Delta = AK'^B$ , where A, B are fitting parameters here.  $K' = q(h/r)^{-0.18}\alpha^{-0.31}$

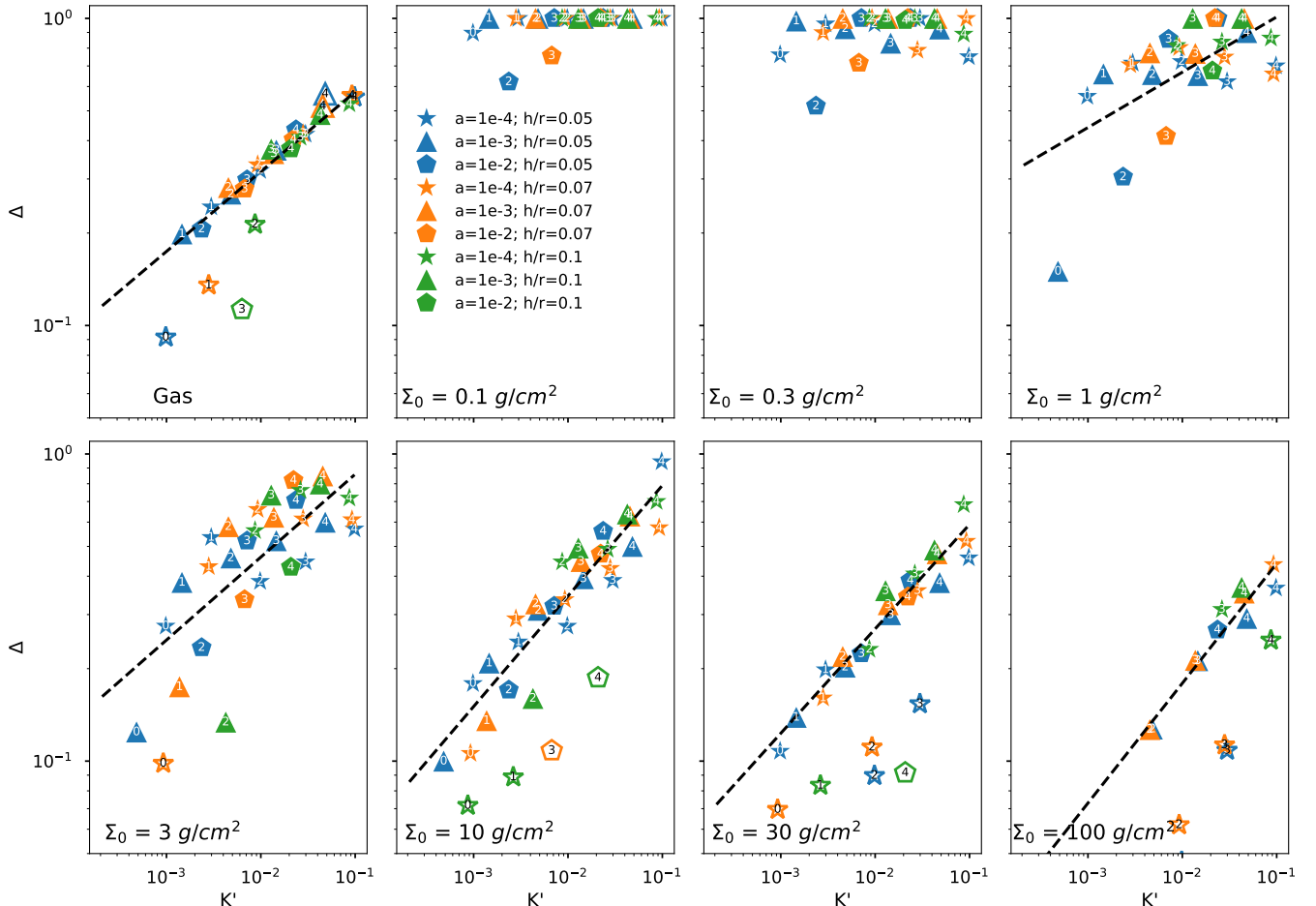


**Figure 7.** Fitting of gap widths  $\Delta$  vs.  $K'$  for different models with dust size distribution  $[s_{max}, p] = [550\text{um}, -3.5]$ . The first panel is the fitting of the gas surface density, which is used to calibrate the index above  $h/r$  and  $\alpha$ . The best fit is  $K' = q(h/r)^{-0.18}\alpha^{-0.31}$  and is shown by the dashed line. and the constants are fitted using equation 10. The stars, triangles, and pentagons represent models of  $a=1e-4$ ,  $1e-3$  and  $1e-2$  respectively. Models for  $h/r = 0.05, 0.07$  and  $0.1$  are in blue, orange and green respectively. The figure 0, 1, 2, 3 and 4 represent the planet mass from 10 Earth mass to 3 Jupiter mass increasingly. We neglect outliers (shown in unfilled markers) when fitting the line. The outliers either have very shallow gaps, or have double gaps (horseshoe in between), thus have widths smaller than their counterparts. The rest of panels are fitting of gaps in dust intensity profile. From left to right and top to bottom, they are models scaled as initial gas density  $= 0.1g/cm^2, 0.3g/cm^2, 1g/cm^2, 3g/cm^2, 10g/cm^2, 30g/cm^2, 100g/cm^2$  at the position of the planet. The definition of  $K'$  are the same as that in the gas surface density (first panel). For the initial gas density  $= 0.1g/cm^2, 0.3g/cm^2$ , the relation is very weak, because most of the gap is so wide that even reaches the inner boundary (Put it another way, the ring is too high.) Thus, we do not seek to find a relation between width and  $K'$  for these two models. For the rest of the model, we fit the points using equation 10 and the constants A and B are shown in Table 2. The best fits are shown in dashed lines.

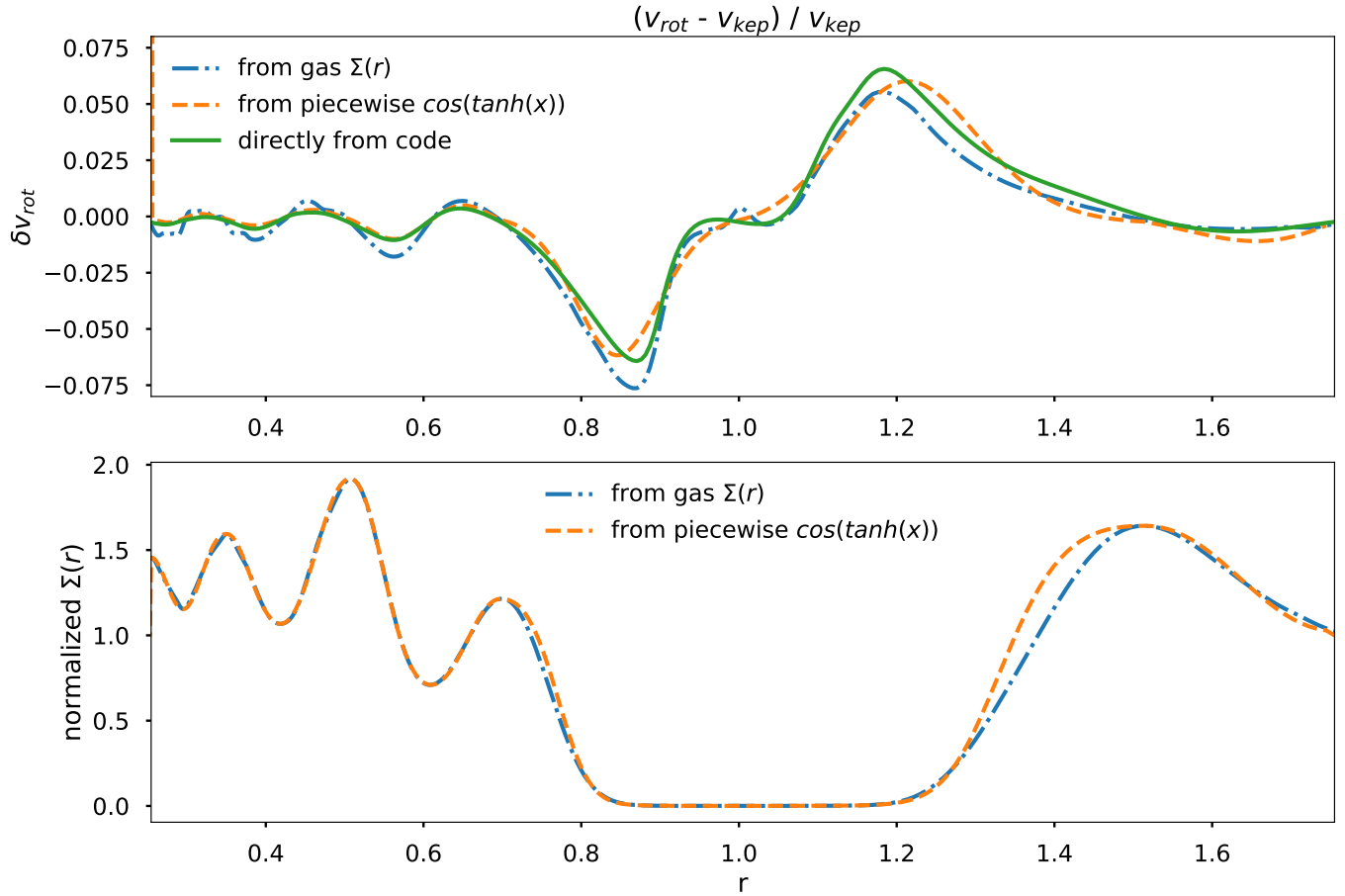


**Figure 8.** The azimuthal velocity from simulations and fittings.

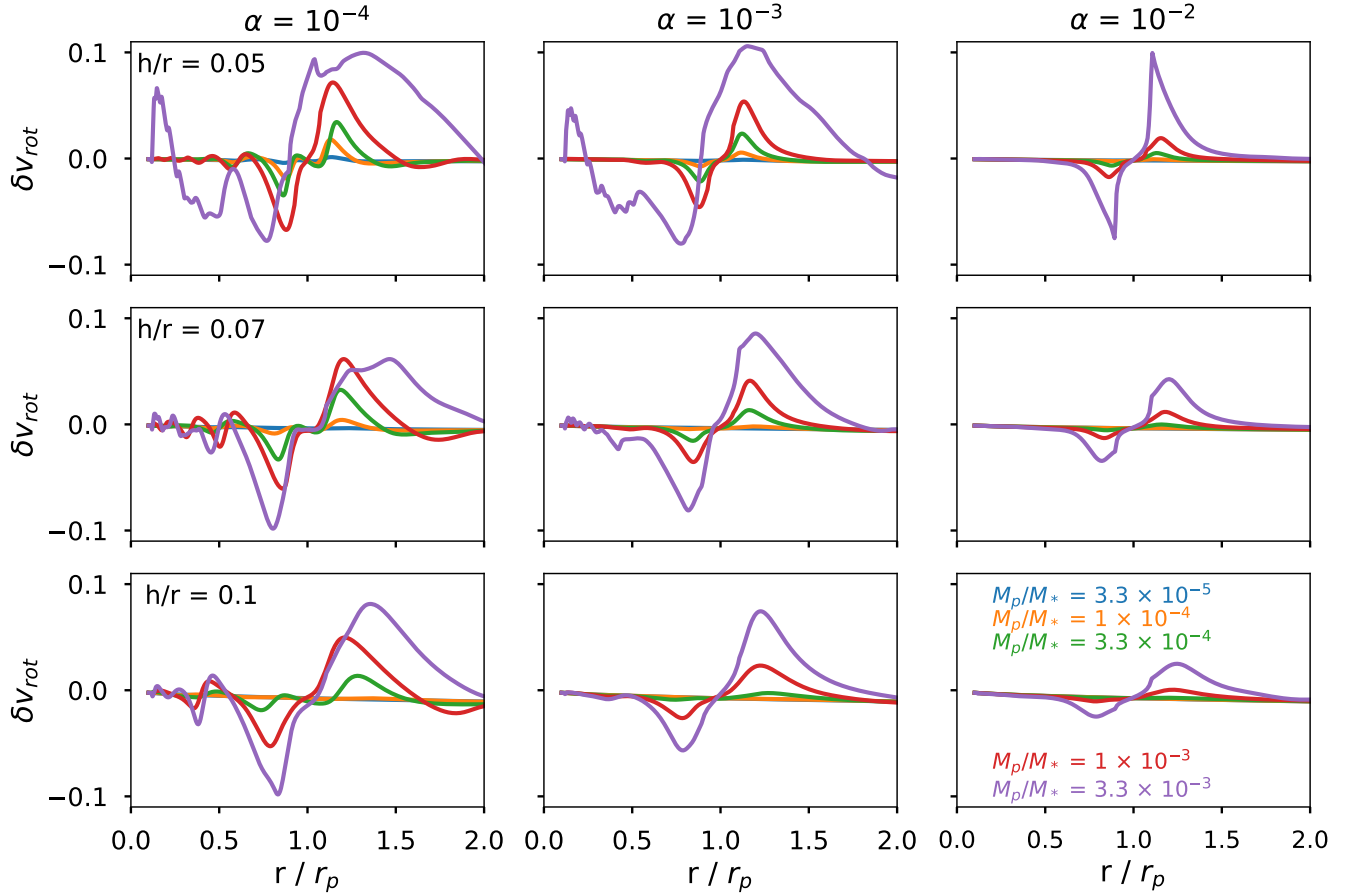


**Figure 9.** The deviation from keplerian velocity for all runs. where  $\delta v_{rot} = (v_{rot} - v_k) / v_k$